A state-selected continuous wave laser excitation method for determining CO2's rotational state distribution in a supersonic molecular beam

Jansen, C.; Juurlink, L.B.F.; Lent, R. van; Chadwick, H.J.

RESEARCH ARTICLE | MAY 17 2024

A state-selected continuous wave laser excitation method for determining CO_2's rotational state distribution in a supersonic molecular beam

Charlotte Jansen ; Ludo B. F. Juurlink ; Richard van Lent ; Helen Chadwick

Rev. Sci. Instrum. 95, 055111 (2024)
https://doi.org/10.1063/5.0203641

Review of Scientific Instruments ARTICLE pubs.aip.org/aip/rsi

A state-selected continuous wave laser excitation method for determining CO_2's rotational state distribution in a supersonic molecular beam

Cite as: Rev. Sci. Instrum. 95, 055111 (2024); doi: 10.1063/5.0203641
Submitted: 15 February 2024 • Accepted: 4 May 2024 •
Published Online: 17 May 2024

Charlotte Jansen,[1,a] Ludo B. F. Juurlink,[1,b] Richard van Lent,[1] and Helen Chadwick[2,c]

AFFILIATIONS

[1] Leiden Institute of Chemistry, Leiden University, P.O. Box 9502, 2300RA Leiden, The Netherlands
[2] Department of Chemistry, Faculty of Science and Engineering, Swansea University, Swansea SA2 8PP, United Kingdom

[a] Author to whom correspondence should be addressed: c.jansen@lic.leidenuniv.nl
[b] l.b.f.juurlink@llinc.leidenuniv.nl
[c] h.j.chadwick@swansea.ac.uk

ABSTRACT

State-resolved experiments can provide fundamental insight into the mechanisms behind chemical reactions. Here, we describe our methods for characterizing state-resolved experiments probing the outcome of the collision between CO_2 molecules and surfaces. We create a molecular beam from a supersonic expansion that passes through an ultra-high vacuum system. The CO_2 is vibrationally excited by a continuous wave infrared (IR) laser using rapid adiabatic passage. We attenuate the fractional excitation using a CO_2 absorption cell in the IR beam path. We combine Monte Carlo simulations and molecular beam energy measurements to find the initial rotational state distribution of the molecular beam. We find that our pure CO_2 beam from a 300 K source has a rotational temperature of ~26 K.

I. INTRODUCTION

Energy-resolved experiments provide detailed insight into the principles underlying the outcomes of gas-surface collisions, i.e., (in)elastic scattering, molecular adsorption, and reactive events. The most common method to control the kinetic energy of the gaseous collision partner makes use of a supersonic molecular beam.[1] Control over the velocity of the molecule of interest is achieved by (anti)seeding the molecule of interest in an inert gas (e.g., He, Ne, or Ar) and varying the nozzle temperature. The rotational distribution of these molecules is generally considered thermalized (although this is not true for hydrogen isotopologues[2]), but there are no general methods to accurately predict the rotational temperature. It depends on the expansion conditions and, likely, on the exact shape of the orifice used to create the supersonic expansion. The vibrational distribution is, on the contrary, generally not thermalized, especially for polyatomic molecules exhibiting multiple energetically clustered states, e.g., CH_4.[3,4] The nozzle temperature used to control the velocity also affects the vibrational and rotational distributions and may be used as a means to separate vibrational and kinetic contributions to scattering[5] and reactivity.[6]

To achieve full state resolution, specific rovibrational states may be populated preferentially using laser excitation of molecules in the molecular beam. For polyatomic molecules, experiments with CH_4[7] (and isotopologues[8]) and D_2O[9] have shown a direct effect of vibrational excitation on sticking and dissociation probabilities on various single crystal surfaces.[9–11] Additional state-selection and detection of scattered CH_4 were also recently shown to be possible and provide detailed information on (in)elastic scattering.[12]

Collisions of CO_2 with surfaces are of interest to a broad range of scientific fields. In astronomy and astrochemistry, CO_2 occurs, for example, in the interstellar medium (ISM)[13] and accretes in ice phases[14] and comets.[15] In the chemical industry, CO_2 is a major reactant in the Cu/ZnO-based catalytic production of methanol. For CO_2, other techniques have been used to study the effect of vibrational excitation on the interaction indirectly.[5,16,17] They use state-resolved detection of desorbing molecules and rely on the principle of detailed balance.

Direct state-resolved measurements of adsorption are challenging for CO_2 and suffer from experimental complexities not appearing, for example, when studying collisions of CH_4. First, CH_4 has been shown to exhibit a (state-resolved) dissociative sticking probability on the order of 10^{-7}–10^{-1}.[18] The dissociative sticking probability of CO_2 is thought to be much lower for Cu—the most relevant metal to industrial catalysis—with reported reaction probabilities ranging from 10^{-11} to 10^{-9}.[19] The review by Burghaus[20] summarizes experimental work performed on CO_2 sticking and reports no indisputable evidence of direct dissociation for any other system. Second, the products of dissociation for CH_4 are readily and uniquely detected by Reflection Absorption Infrared Spectroscopy (RAIRS).[21] For CO_2, the easily detectable product CO is always present as a contaminant in both the CO_2 gas source and the vacuum background. Since CO has a sticking probability that exceeds that of CO_2 by many orders of magnitude,[22–24] it may dominate the signal and hide the actual reactivity of CO_2. Third, the presence of CO_2 in the air complicates the experiment compared to CH_4. When an excitation laser is tuned to a rovibrational transition in CO_2, it is absorbed to a significant extent by CO_2 molecules naturally present in the air. Both the relatively high partial pressure in the air in comparison to the supersonic molecular beam and the orders of magnitude difference in path length (meters outside the vacuum system vs millimeters in the molecular beam) require that the entire laser beam path be purged or evacuated. Finally, the commercially available cw-laser systems that may excite stretch and bend vibrations in CO_2 in a state-resolved manner have an output power in the required frequency range that is approximately one order of magnitude lower than those available to excite several vibrations in CH_4. For isotopically labeled CO_2, the power output is lowered even more and yields issues with frequency stabilization.

Here, we describe the methods that have recently enabled us to perform full energy-selected gas-surface collision experiments for CO_2.[25] They are very similar to earlier described methods that focused on CH_4 and D_2O[26] but were adapted to work for CO_2. We show how we determine the rotational temperature and total excited population of CO_2 in the molecular beam. This is necessary for quantifying state-resolved adsorption and reaction probabilities. We measure the change in energy in the molecular beam due to laser excitation as described previously by McCabe *et al.*[27] and compare the results to Monte Carlo simulations as performed by Chadwick *et al.*[28]

II. EXPERIMENTAL

A. Setup

Our experiments are performed using a home-built ultra-high vacuum (UHV) system that has been used for reaction dynamics measurements of several different molecules, including H_2/D_2, O_2, and CO.[29–32] It consists of three differentially pumped chambers for the creation of a molecular beam and an analysis chamber with a base pressure of 2×10^{-10} mbar. Figure 1 shows a schematic illustration of the apparatus in two possible configurations.

The molecular beam is created by expanding high-purity CO_2 (Linde Gas, purity 5.3), which can be seeded with high-purity He (Linde Gas, purity 6.0). Flow controllers feed the gas at 4–7 bars into a vacuum chamber ($<1 \times 10^{-3}$ mbar) through a 28 μm circular orifice in a tungsten nozzle. The nozzle can be heated up to 1100 K

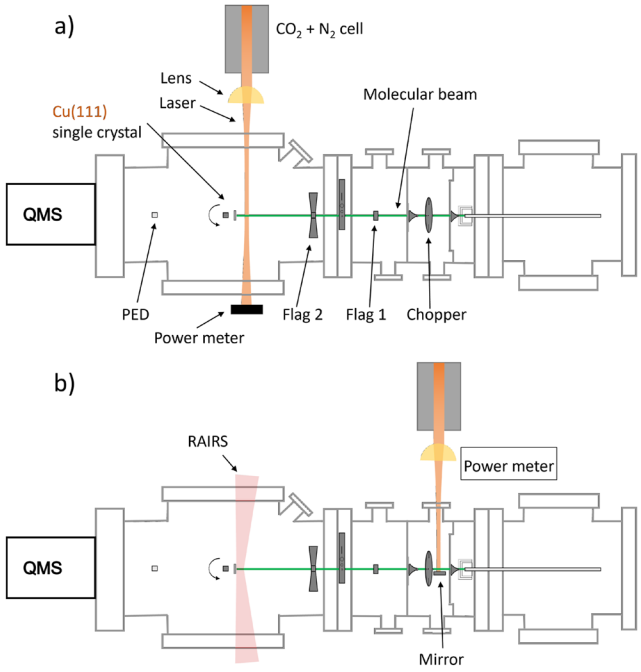

FIG. 1. The UHV system in two possible configurations, showing the four connected vacuum chambers, the molecular beam, the beam chopper, flags and sliding valve, the sample, the position of the excitation laser, and several measurement devices, such as a quadrupole mass spectrometer (QMS), pyroelectric detector (PED), reflection absorption infrared spectrometer (RAIRS), and laser power meter. In configuration (a), the excitation laser is located in the main analysis chamber. Due to the short travel time from vibrational excitation to the sample, virtually no vibrational energy is lost via spontaneous emission. In configuration (b), the excitation laser is moved to make room for a RAIRS spectrometer and to prevent stray laser light from directly influencing the PED measurement. The longer distance between excitation and experiment (about 0.5 m) does cause a loss of the excited population of 10%–30%, depending on molecular velocity.

to vary the kinetic energy and rotational and vibrational temperature of the beam. For the experiments described here, only pure CO_2 gas is used at room temperature.

Two skimmers and a third orifice shape the molecular beam, resulting in a molecular beam with a narrow angular spread. The angular spread can be varied by switching the third orifice, which is located in a sliding valve. The sliding valve contains three circular orifices of varying diameters and a single narrow slit used for position-dependent measurements on curved crystals.[29,30] During the expansion, kinetic and rotational energy is converted to translational energy along the beam axis, resulting in a low rotational temperature and low transverse velocity of the molecules within the beam. The average beam velocity is determined by time-of-flight (TOF) spectrometry and is found to be 587 m/s with a full width at half maximum of ~130 m/s for a pure CO_2 beam at a nozzle temperature of 300 K. This corresponds to the beam having a translational temperature of ~30 K. The full velocity distribution can be found in the supplementary material of a previous article.[25]

After leaving the source chamber, the molecular beam travels through two differentially pumped vacuum chambers before entering the UHV analysis chamber. In the first chamber, a high-speed

chopper wheel allows us to create short gas pulses from the molecular beam for TOF spectrometry. When not in use, the wheel can be manually set to the "open" position. In configuration (b) in Fig. 1, this chamber is also the location of the CO_2 excitation laser. The second differentially pumped chamber contains a flag that can block the beam from hitting the sliding valve and entering the main chamber. This flag can be opened and closed rapidly to create a modulated molecular beam. Typical modulation frequencies are on the order of 1 Hz.

In the main chamber, there is an x, y, z, and θ manipulator with a sample mounted to the bottom of a liquid nitrogen (LN_2) cryostat. The temperature of the sample is monitored by a K-type thermocouple and is controlled by radiative heating and electron bombardment using a filament (Osram) at the back of the sample.

Just past the entrance of the main chamber, a second flag can block the beam from directly hitting the sample surface. The surface of the flag is slanted so as not to reflect the molecular beam back into the previous chamber. The two beam flags combined allow us to perform King and Wells-type sticking probability measurements.[33] They are labeled in Fig. 1(a). In configuration (b) in Fig. 1, the sample surface can also be monitored using an FTIR (Bruker Vertex 70) for RAIRS experiments in combination with laser excitation of the CO_2.

Behind the crystal, a moveable room-temperature bolometer (pyro-electric detector, Eltec model 406) is used to quantify the vibrational excitation of CO_2 molecules on the molecular beam axis. At the end of the main chamber, a quadrupole mass spectrometer (QMS) on the molecular beam axis is used to perform TOF measurements.

We use infrared laser light from an optical parametric oscillator (OPO) (Argos model 2400, module D) to vibrationally excite CO_2 in the molecular beam. The D module of the OPO has an output wavelength range of 3.9–4.6 μm, with output power ranging from >1 W around 4 μm to less than 100 mW at the higher wavelengths. At the wavelength of the ν_3 asymmetric stretch vibration of CO_2 around 4255 nm, a typical output power is 200–300 mW. A beam splitter directs half of the power to the molecular beam and half of the power to the wavelength stabilization system. The stabilization system consists of a CO_2 reference cell with a mirror at the end and an MCT detector (Thorlabs PDAVJ5). The reflected light travels through the reference cell twice and shows a Lamb dip in the absorption spectrum, which is measured by the MCT detector. A LaseLock system (TEM Messtechnik) locks the laser wavelength to the center of the Lamb dip by Piezo control of the OPO seed laser. The wavelength is also monitored with a wavemeter (Bristol model 621).

The entire path of the laser is purged with dry N_2, as background CO_2 and H_2O can destabilize the OPO, and CO_2 will absorb the laser light before it reaches the vacuum chamber. This means all optical equipment is enclosed and cannot be accessed during measurements without disturbing the N_2 atmosphere.

When attenuating laser power, a manual polarization-based attenuator cannot be used easily in a purged environment. A motorized polarization-based attenuator can be used, but this can be expensive. They are also complicated to set up as they require a second polarizer, and if not installed correctly, they can lead to slight changes in laser alignment as the polarizer is rotated, which can cause an increase (or decrease) in signal not related to the laser power. Here, we present an alternative, relatively simple method that can be implemented in various ways with materials readily available in most laboratories. We use the CO_2 absorption to our advantage and use a CO_2 gas cell in the path to the vacuum system to attenuate the laser light. It is shown and labeled in both Figs. 1(a) and 2. The cell is made of a stainless steel tube with a gas line connection and infrared (IR) viewports on both ends. It is normally continuously purged using dry N_2 from an in-house system originating from the exhaust of the local nuclear magnetic resonance (NMR) facilities. When we need to attenuate the laser, we use a flow controller to dose additional CO_2 into the gas line. The cell is then "purged" with the N_2 + CO_2 mixture, and the laser attenuation depends on the concentration of CO_2. There are other ways of implementing this idea, such as using a vacuum cell that can be filled with CO_2 or air. Depending on the available materials, an additional advantage of this method could be that laser power loss can be minimized, for example, by using Brewster angle windows on the cell. Note that the method only works on laser wavelengths resonant with CO_2. Since we only use resonant wavelengths in our experiments, this is not a disadvantage and can even be helpful as it can indicate errors such as the laser accidentally drifting off-resonance.

After the attenuation cell, a cylindrical lens (ZnSe, focal length of 200 mm) in the path of the laser is used to achieve rapid adiabatic passage, where the curved wavefronts of the focused laser create a

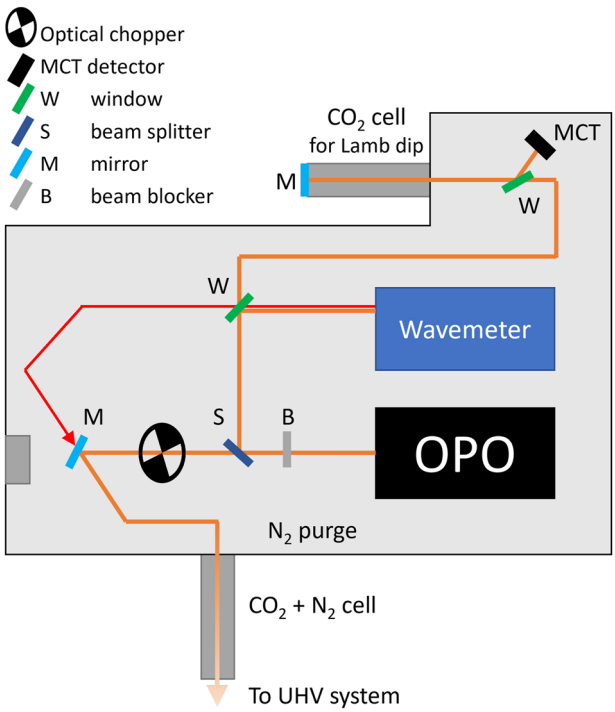

FIG. 2. The setup of the laser system. It consists of an OPO with variable wavelength output (orange), a stabilization system, an alignment laser (red), and a CO_2 + N_2 attenuation cell. The attenuation cell is described in more detail in the text. The stabilization system uses the Lamb dip measured in a CO_2 cell to lock the OPO to a chosen CO_2 absorption wavelength. The whole system is purged with N_2 to prevent destabilization by H_2O and CO_2 and unwanted absorption by CO_2.

frequency sweep experienced by the traveling molecules due to the Doppler effect.[28,34] This allows the excited population at any given rovibrational level to exceed 50%. Given enough laser power, full population inversion can be achieved.[28]

B. Measuring laser excitation

For a given rovibrational excitation, the required laser frequency varies depending on the initial vibrational and rotational states. Due to the narrow bandwidth (<1 MHz) of the laser, vibrations can only be excited from a single initial rovibrational state. We use a pure CO_2 beam with a nozzle temperature of 300 K. At this temperature, most molecules are in the vibrational ground state.[35] However, at 300 K, many rotational states are populated. During the expansion of the molecular beam, part of the rotational energy is converted to kinetic energy, which narrows the distribution of rotational states. When quantifying the results of state-resolved experiments, it is important to know what fraction of the molecules can be excited by the state of interest. Therefore, it is necessary to know what fraction of the molecules are initially in the vibrational and rotational states that will be excited by the laser.

Here, we excite the R(0) to R(10) transitions of the ν_3 asymmetric stretch vibration. For CO_2 in the vibrational ground state, there are only even rotational states due to the Pauli exclusion principle. We use configuration (a) in Fig. 1. We measure the rovibrational excitation of CO_2 molecules in a molecular beam with the pyroelectric detector (PED, Eltec Model 406) in the molecular beam path. This detector responds to changes in temperature caused by energy transfer from the molecular beam to the detector. A change in the internal energy of the CO_2 due to vibrational excitation will be visible in the PED signal. Due to the limited width of the PED, the spread of the measured part of the molecular beam is 0.15°. The first flag in the molecular beam path is used to modulate the molecular beam since the PED is only sensitive to changing input. The PED signal is amplified and converted to a DC signal by a lock-in amplifier (AMETEK Model 5210).

During the measurement, we continuously measure the laser power with a thermal power meter (Thorlabs S302C) behind a sapphire exit window in the vacuum chamber. We vary the laser power with the N_2 + CO_2 cell in the laser path by varying the partial pressure of CO_2 in the cell. The gas cell only attenuates the laser light resonant with the CO_2 vibration, and we found that a small fraction (5 mW) of the laser light was not resonant with the transition. We expect the measured excitation to initially increase linearly at low laser power before reaching an asymptote at higher laser power.

C. Simulations

The excited population as a function of laser power can also be determined using simulations. Here, we use the same Monte Carlo simulations as Chadwick *et al.*,[28] where the optical Bloch equations are solved for conditions similar to the experiment. The original code was written for CH_4 and took into account the angular spread of the molecular beam, the velocity distribution of the molecules, and the curved laser wavefronts for rapid adiabatic passage. We also take into account the different interaction strengths of different m_j states with the laser, determined by their Clebsch–Gordan (CG) coefficients, shown in Table I. We assume the distribution of m_j states is uniform. Previous research has suggested that the molecules in a molecular beam may not be randomly oriented due to collisions between molecules in the beam.[36] However, they found that this effect was strongest in seeded molecular beams. Since we use a pure beam, we expect this effect to be small and do not take it into account.

The interaction strength between the molecule and electric field is characterized by the Rabi frequency,[37]

$$\Omega = \frac{\vec{\mu} \cdot \vec{E}}{\hbar}, \tag{1}$$

where $\vec{\mu}$ is the transition dipole moment and $\vec{E}$ is the electric field. The m_j state dependence via the CG coefficients is included in $\vec{\mu}$.[28] Equation (1) shows that the interaction strength also depends on the orientation of the molecule with respect to the electric field. For CH_4, the orientation of the molecule is irrelevant as the molecule is spherically symmetric. For CO_2, this is not the case, as the transition dipole moment is fixed along the bond axis for the asymmetric stretch vibration. Therefore, we have to take into account the orientation of the transition dipole moment $\vec{\mu}$ of the molecule with respect to the electric field, which is in this case defined by the laser polarization.

We rewrite Eq. (1) to separate the calculation of the dot product from the rest of the equation for easier implementation in the simulations,

$$\Omega = \frac{A \times \mu \times E}{\hbar}, \tag{2}$$

$$A = |\hat{\mu} \cdot \hat{E}|, \tag{3}$$

where $\hat{E}$ is a unit vector along the laser polarization axis. A detailed explanation of how we calculate A is provided in the supplementary

TABLE I. The Clebsch–Gordan coefficients used in the simulations.

	m = ±0	m = ±1	m = ±2	m = ±3	m = ±4	m = ±5	m = ±6	m = ±7	m = ±8	m = ±9	m = ±10
j = 0	1.0										
j = 2	0.77	0.73	0.58								
j = 4	0.75	0.73	0.68	0.6	0.45						
j = 6	0.73	0.73	0.7	0.66	0.6	0.51	0.38				
j = 8	0.73	0.72	0.71	0.69	0.65	0.6	0.54	0.46	0.33		
j = 10	0.72	0.72	0.71	0.7	0.67	0.64	0.61	0.56	0.5	0.42	0.3

material. We find that for a distribution of randomly oriented non-rotating molecules, A has a uniform distribution between 0 and 1.

For all rotational states besides $J = 0$, the orientation of the molecule is not fixed. The molecules complete millions of rotations during their path through the laser beam. We take this into account by calculating the average value of the effective transition dipole moment during a full rotation. This changes the distribution of A to a nonuniform distribution from 0 to $\pi/2$, which favors the higher values. A detailed derivation of this result can also be found in the supplementary material.

For every iteration of the simulation, a value is chosen from the distributions of each of the aforementioned parameters. In total, 1000 iterations are averaged for each simulated laser power.

III. RESULTS AND DISCUSSION

Figure 3(a) shows how the PED signal varies as a function of laser power for the R(6) transition. The gray dashed line shows the average PED signal when there is no vibrational excitation. This signal is mostly due to the kinetic energy of the molecules. As the laser power increases, so does the PED signal, indicating that there is laser-induced vibrational excitation. There are no data below 5 mW due to a small amount of non-resonant laser light present in the laser beam. The data show some outliers and gaps. The outliers are due to the slow response time of the lock-in amplifier when the laser power was varied too quickly. To mitigate this issue, the laser power was kept constant for a while before moving to the next value. There are gaps because the laser power could not be varied in a controlled way due to the method used to attenuate the laser. Around 30 mW, there is a small cluster of data points on the gray line. This shows a point in the measurement where the laser was off the resonant frequency; the laser power was relatively high, but there was no excitation. Figure 3(b) shows the data for all measurements. The apparent asymptote of the PED signal varies between the different transitions. This is due to the different populations of the initial state of each transition. We will use this later to calculate the rotational state distribution and rotational temperature of the molecular beam.

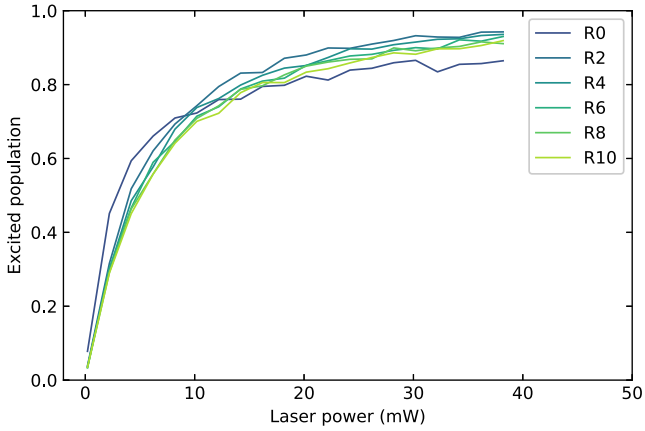

FIG. 4. The result of all simulations for R(0) to R(10). The graph shows the excited population normalized to the initial population as a function of laser power. Note that excited populations above 50% can be achieved due to rapid adiabatic passage.

Figure 4 shows the results of the simulations for the pure CO_2 beam for each transition from R(0) to R(10). It shows the fraction of the initial population that finishes in the excited state after passing through the laser field. These results are obtained separately for each initial rotational state and do not take into account the distribution of rotational states in the molecular beam.

A. Obtaining the rotational state distribution

The rotational state distribution can be obtained by fitting the experimental data with the simulation results. For the experiment, the signal value depends on the number of molecules available in

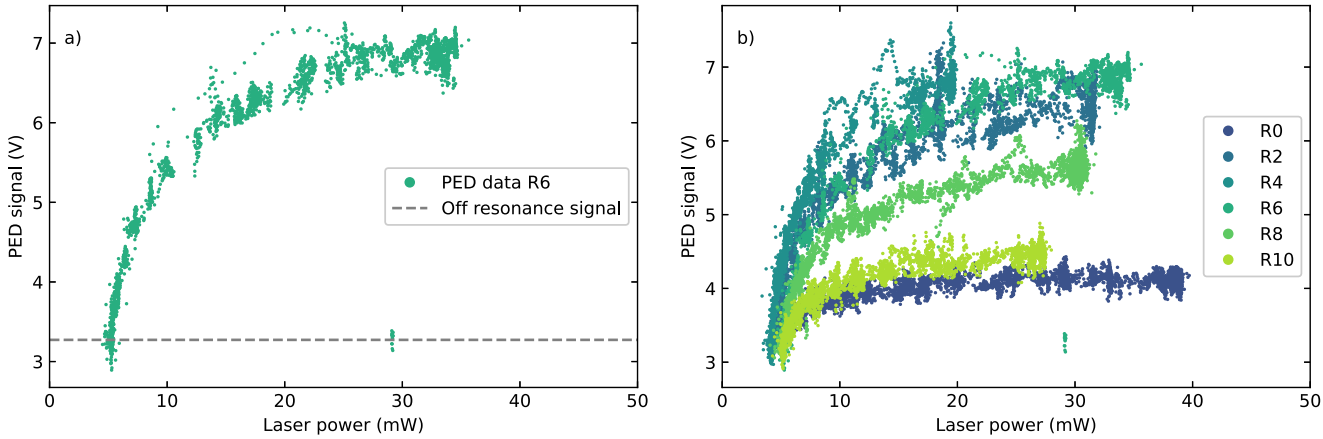

FIG. 3. The signal of the pyroelectric detector (PED), which is a measure for the amount of vibrational excitation, as a function of laser power. The increase in signal starts around 5 mW because there is a small amount of non-resonant laser light present that could not be attenuated during the experiment. (a) A single dataset. The gray dashed line shows the PED signal without excitation. The small cluster of data points on the gray line around 30 mW shows a point during the measurement where the laser was off-resonance. (b) All measured datasets.

the initial state; the more molecules are available to be excited, the higher the final PED signal will be. The signal will, therefore, vary between different initial rotational states depending on the relative population of each rotational state. This can be seen in Fig. 3(b).

We determine the relative populations of each rotational state by fitting the experimental data with the simulation results. The data are normalized to the off-resonance signal to correct for any small differences in experimental conditions, such as in PED position/sensitivity or beam flux. The off-resonance signal is mostly from the kinetic energy of the molecular beam. Then, the off-resonance signal is subtracted from the data, so only the normalized, on-resonance signal is left. The simulation results are fitted to the data using three fit parameters. The first two are effective corrections to the measured laser power to more accurately portray the effective laser power at the molecular beam position. The first is the amount of off-resonance laser light in the laser beam. This is ~5 mW, but it varies between measurements, and its exact value for each measurement is determined by the fit. The second parameter is the loss of power between the molecular beam and the power meter in the system. This is due to the exit window of the vacuum chamber and a small pocket of air between the window and the power meter. We assume the loss percentage is the same for each measurement, and the fit parameter is forced to have the same value for all datasets. The third and most important fit parameter is the scaling amplitude of the simulation results; this parameter is directly related to the relative populations of the rotational states in the molecular beam.

Figure 5(a) shows the PED data and the resulting fits with the simulation data for all measured rotational transitions [R(0) to R(10)]. Every dataset has the off-resonance PED signal removed and is normalized to the off-resonance signal to correct for any sensitivity variations between measurements. The datasets are all shifted horizontally to remove the fraction of laser power that is due to non-resonant laser light (around 5 mW, but varying between experiments and depending on the fit). Furthermore, the laser power is corrected for the losses in the exit window and air pocket. The difference in signal amplitude between the different rotational states is clearly visible. The scaling amplitudes for the fit of all rotational states, which are related to the relative populations of the rotational states, are shown in Fig. 5(b). To calculate the rotational temperature of the molecular beam, we fit these amplitudes with the rotational partition function,

$$A(2J+1)e^{\frac{-J(J+1)\Theta_r}{T}}, \tag{4}$$

where J is the initial rotational state, T is the temperature, and Θ_r is a molecule-specific constant depending on the moment of inertia of the molecule. For CO_2, its value is 0.561 K.[38] We find that this function fits well with our measured populations, and we find a rotational temperature of 26 ± 1.4 K. The error is based on the final fit of the rotational temperature. There are errors associated with several parameters earlier in the data analysis process that are difficult to calculate, such as errors in simulation parameters and the fit of the simulated data to the measured data. We estimate these could cause an error of a few Kelvin on the reported rotational temperature of the beam. After the fit, both the Boltzmann function and the measured populations are normalized by dividing by the partition function to get absolute values for the fraction of the beam that is in each rotational state. Here, we also take into account that 8% of the molecules are not in the vibrational ground state (see supplementary material).

These rotational state populations can be combined with the results of the simulations to calculate the absolute fraction of the molecular beam that is excited by the laser for a given laser power. Depending on the distance from the excitation laser to the sample, spontaneous emission may also affect the excited population significantly. When necessary, we can easily correct this using the velocity of the molecular beam and the lifetime of the excited state.

The rotational temperature of CO_2 molecular beams has been determined before by Perkins and Nesbitt.[17] They found rotational temperatures of the vibrational ground state of ~18 ± 3 K, with very little variation between different molecular beam mixtures

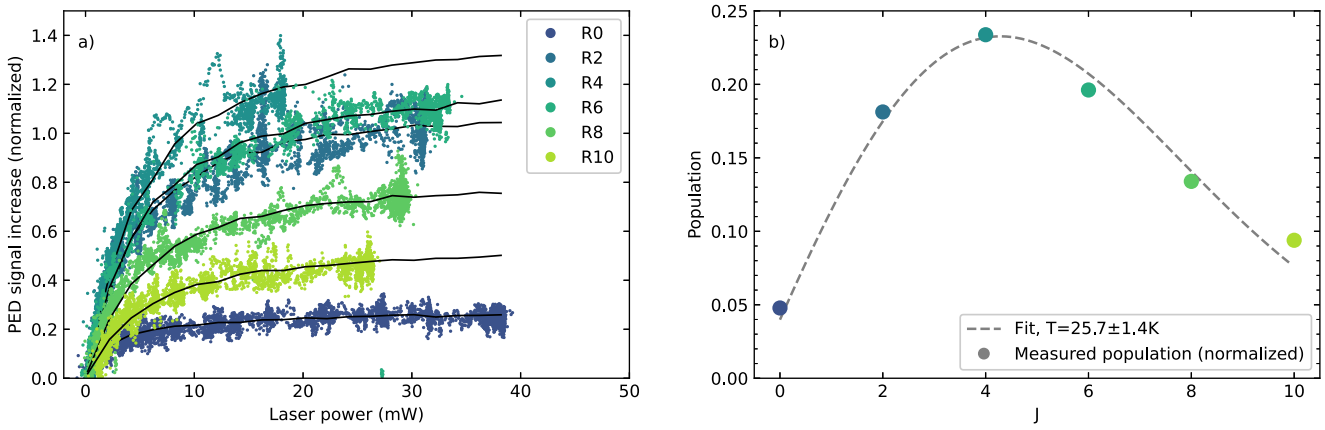

FIG. 5. (a) The normalized and shifted PED data for all measured transitions and the corresponding simulation result scaled according to the fit. The difference in signal increase between the different initial rotational states is clearly visible. (b) The population of each initial J state, calculated from the scaling factors of the fits in (a) and normalized using the partition function calculated using a fit [dashed line, Eq. (4)].

(10% CO_2 in Ar, Ne, He, and H_2). Our rotational temperature of 26 K is similar, though slightly higher. The difference could be explained by the fact that we use a pure CO_2 beam or by the difference in expansion conditions. Clustering of the CO_2 molecules in the pure beam could affect the (rotational) cooling of the molecular beam. However, we did not see any evidence of clustering in our beam. Perkins and Nesbitt use a pulsed molecular beam with a nozzle diameter of 500 μm. Our nozzle diameter is 28 μm. The quality of the supersonic expansion typically depends on the product P_0D, where P_0 is the gas pressure in the nozzle and D is the nozzle diameter. In our experiment, this product is ~2 times larger than in the experiment of Perkins and Nesbitt. However, the higher rotational temperature of the molecular beam indicates that the quality of the expansion is lower. This might be caused by the geometry of the nozzle. For a small-diameter nozzle, the length of the orifice is typically larger with respect to its diameter. Angled walls of the orifice result in a more extreme cone shape for a longer orifice than a shorter one. It is also possible that the shape of our small orifice is less regular than that of a large orifice. The supplementary material shows an image of the 28 μm nozzle orifice. The effective shape may also be changed during experiments by debris in the nozzle. These differences may affect the expansion and (rotational) cooling of the molecular beam.

It is also interesting to compare the two techniques that have been used to obtain a rotational temperature for a CO_2 molecular beam, i.e., those presented here with linear absorption spectroscopy. While linear absorption spectroscopy is, at least in principle, a simpler technique to implement, it would not be possible to use it here due to the inherent instability of the power of the laser system used (<5% root mean square fluctuations), which we estimate is two orders of magnitude larger than that which would be absorbed by the molecules. Instead of using absorption, the results presented here suggest that the pyroelectric detector signal could be used instead. As shown in Fig. 4, the simulated fluence curves have the same gradient at low laser powers for all the transitions probed and, therefore, the ratio of the measured pyroelectric detector signals at a given, sufficiently low laser power would also give a rotational temperature. This would again be difficult to achieve experimentally in the current work due to the method used for attenuating the laser power, which would make measuring the pyroelectric detector signal at the same laser power for each transition challenging. We, therefore, believe that the methodology presented here provides an alternative method for determining the rotational temperature of a molecular beam when the laser power fluctuates significantly more than the measured absorption and in circumstances where it is difficult to produce the same (low) laser power for different transitions as would be necessary.

IV. SUMMARY

We used laser excitation to excite the R(0) to R(10) transitions of the ν_3 vibration in CO_2. We measured the excitation with a pyroelectric detector and compared the results with Monte Carlo simulations. We have quantified state-resolved vibrational excitation in CO_2 molecules in a molecular beam and determined that the rotational temperature of the pure CO_2 molecular beam is 26 K. This result can be used to quantify the results of other state-resolved measurements, such as sticking probability measurements using the King and Wells method.[33] We used it to quantify an upper limit for the effect of vibrational excitation on CO_2 physisorption on CO_2 ice.[25]

SUPPLEMENTARY MATERIAL

The supplementary material contains the calculation of the vibrational ground state population in the molecular beam, elaborate calculations of the distributions of molecular orientations in the beam, and an electron microscope image of the nozzle used for the molecular beam.

ACKNOWLEDGMENTS

This work was part of the research program Materials for Sustainability with Project No. 739.017.008, which is (partly) financed by the Dutch Research Council (NWO). Grammarly has been used to correct spelling and grammar.

AUTHOR DECLARATIONS

Conflict of Interest

The authors have no conflicts to disclose.

Author Contributions

Charlotte Jansen: Conceptualization (supporting); Investigation (lead); Methodology (equal); Software (equal); Writing – original draft (lead); Writing – review & editing (equal). **Ludo B. F. Juurlink**: Conceptualization (lead); Methodology (equal); Supervision (lead); Writing – review & editing (equal). **Richard van Lent**: Methodology (equal); Writing – review & editing (equal). **Helen Chadwick**: Software (equal); Supervision (supporting); Writing – review & editing (equal).

DATA AVAILABILITY

The data that support the findings of this study are available from the corresponding author upon reasonable request.

REFERENCES

[1] A. W. Kleyn, "Molecular beams and chemical dynamics at surfaces," Chem. Soc. Rev. **32**(2), 87–95 (2003).
[2] J. E. Pollard, D. J. Trevor *et al.*, "Rotational relaxation in supersonic beams of hydrogen by high resolution photoelectron spectroscopy," J. Chem. Phys. **77**(10), 4818–4825 (1982).
[3] D. K. Bronnikov, P. V. Zyrianov, D. V. Kalinin, Y. G. Filimonov, A. W. Kleyn, and J. C. Hilico, "A diode laser spectrometer for state-resolved experiments on the methane-surface system," Chem. Phys. Lett. **249**(5-6), 423–432 (1996).
[4] D. K. Bronnikov, D. V. Kalinin, V. D. Rusanov, Y. G. Filimonov, Y. G. Selivanov, and J. C. Hilico, "Spectroscopy and non-equilibrium distribution of vibrationally excited methane in a supersonic jet," J. Quant. Spectrosc. Radiat. Transfer **60**(6), 1053–1068 (1998).

[5]S. J. Sibener and Y. T. Lee, "The internal and translational energy dependence of molecular condensation coefficients: SF_6 and CCl_4," J. Chem. Phys. **101**(2), 1693–1703 (1994).
[6]C. T. Rettner, D. J. Auerbach, and H. A. Michelsen, "Role of vibrational and translational energy in the activated dissociative adsorption of D_2 on Cu(111)," Phys. Rev. Lett. **68**(8), 1164–1167 (1992).
[7]L. B. F. Juurlink, P. R. McCabe, R. R. Smith, C. L. DiCologero, and A. L. Utz, "Eigenstate-resolved studies of gas-surface reactivity: CH_4 (ν_3) dissociation on Ni(100)," Phys. Rev. Lett. **83**(4), 868–871 (1999).
[8]P. M. Hundt, H. Ueta, M. E. van Reijzen, B. Jiang, H. Guo, and R. D. Beck, "Bond-selective and mode-specific dissociation of CH_3D and CH_2D_2 on Pt(111)," J. Phys. Chem. A **119**(50), 12442–12448 (2015).
[9]P. M. Hundt, B. Jiang, M. E. van Reijzen, H. Guo, and R. D. Beck, "Vibrationally promoted dissociation of water on Ni(111)," Science **344**(6183), 504–507 (2014).
[10]L. B. F. Juurlink, R. R. Smith, and A. L. Utz, "The role of rotational excitation in the activated dissociative chemisorption of vibrationally excited methane on Ni(100)," Faraday Discuss. **117**, 147–160 (2000).
[11]L. Chen, H. Ueta, R. Bisson, and R. D. Beck, "Vibrationally bond-selected chemisorption of methane isotopologues on Pt(111) studied by reflection absorption infrared spectroscopy," Faraday Discuss. **157**, 285 (2012).
[12]J. Werdecker, B.-J. Chen, M. E. Van Reijzen, A. Farjamnia, B. Jackson, and R. D. Beck, "State-to-state methane-surface scattering as a probe of catalytic activity," Phys. Rev. Res. **2**(4), 043251 (2020).
[13]L. B. d'Hendecourt and M. Jourdain de Muizon, "The discovery of interstellar carbon dioxide," Astron. Astrophys. **223**, L5–L8 (1989).
[14]E. F. van Dishoeck, "ISO spectroscopy of gas and dust: From molecular clouds to protoplanetary disks," Annu. Rev. Astron. Astrophys. **42**, 119–167 (2004).
[15]D. Despois, N. Biver, D. Bockelée-Morvan, and J. Crovisier, "Observations of molecules in comets," Proc. Int. Astron. Union **1**(S231), 469–478 (2005).
[16]M. J. Weida, J. M. Sperhac, and D. J. Nesbitt, "Sublimation dynamics of CO_2 thin films: A high resolution diode laser study of quantum state resolved sticking coefficients," J. Chem. Phys. **105**(2), 749 (1996).
[17]B. G. Perkins and D. J. Nesbitt, "Quantum-state-resolved CO_2 scattering dynamics at the gas-liquid interface: Incident collision energy and liquid dependence," J. Phys. Chem. B **110**(34), 17126–17137 (2006).
[18]R. D. Beck and T. R. Rizzo, "Quantum state resolved studies of gas/surface reaction dynamics," Chimia **58**(5), 306 (2004).
[19]J. Nakamura, J. A. Rodriguez, and C. T. Campbell, "Does CO_2 dissociatively adsorb on Cu surfaces?," J. Phys.: Condens. Matter **1**(SB), SB149–SB160 (1989).
[20]U. Burghaus, "Surface chemistry of CO_2—Adsorption of carbon dioxide on clean surfaces at ultrahigh vacuum," Prog. Surf. Sci. **89**(2), 161–217 (2014).
[21]H. Ueta, L. Chen, and R. D. Beck, "State-resolved methane dissociation on Pt(111) studied by reflection absorption infrared spectroscopy," J. Surf. Sci. Soc. Jpn. **36**(12), 614–619 (2015).
[22]S. Kneitz, J. Gemeinhardt, and H. P. Steinrück, "A molecular beam study of the adsorption dynamics of CO on Ru(0001), Cu(111) and a pseudomorphic Cu monolayer on Ru(0001)," Surf. Sci. **440**(3), 307–320 (1999).
[23]J. Liu, M. Xu, T. Nordmeyer, and F. Zaera, "Sticking probabilities for CO adsorption on Pt(111) surfaces revisited," J. Phys. Chem. **99**(16), 6167–6175 (1995).
[24]J. T. Kindt and J. C. Tully, "Dynamical corrugation: Simulations of the sticking of CO on Cu(100)," Surf. Sci. **477**(2–3), 149–162 (2001).
[25]C. Jansen and L. B. F. Juurlink, "State-resolved studies of CO_2 sticking to CO_2 ice," Front. Chem. **11**, 1250711 (2023).
[26]H. Chadwick and R. D. Beck, "Quantum state–resolved studies of chemisorption reactions," Annu. Rev. Phys. Chem. **68**(1), 39–61 (2017).
[27]P. R. McCabe, L. B. F. Juurlink, and A. L. Utz, "A molecular beam apparatus for eigenstate-resolved studies of gas-surface reactivity," Rev. Sci. Instrum. **71**(1), 42–53 (2000).
[28]H. Chadwick, P. M. Hundt, M. E. van Reijzen, B. L. Yoder, and R. D. Beck, "Quantum state specific reactant preparation in a molecular beam by rapid adiabatic passage," J. Chem. Phys. **140**(3), 034321 (2014).
[29]R. van Lent, S. V. Auras, K. Cao, A. J. Walsh, M. A. Gleeson, and L. B. F. Juurlink, "Site-specific reactivity of molecules with surface defects—The case of H_2 dissociation on Pt," Science **363**(6423), 155–157 (2019).
[30]C. Jansen and L. Juurlink, "Absolute dissociation cross sections for D_2 dissociation on Pt steps," Chem. Phys. Lett. **776**, 138679 (2021).
[31]K. Cao, R. van Lent, A. W. Kleyn, and L. B. F. Juurlink, "A molecular beam study of D_2 dissociation on Pt(111): Testing SRP-DFT calculations," Chem. Phys. Lett. **706**, 680–683 (2018).
[32]D. Zhang, C. Jansen, A. W. Kleyn, and L. B. F. Juurlink, "Adsorption dynamics of O_2 on Cu(111): A supersonic molecular beam study," Phys. Chem. Chem. Phys. **25**(21), 14862–14868 (2023).
[33]D. A. King and G. Wells, "Molecular beam investigation of adsorption kinetics on bulk metal targets: Nitrogen on tungsten," Surf. Sci. **29**(2), 454–482 (1972).
[34]N. V. Vitanov, T. Halfmann, B. W. Shore, and K. Bergmann, "Laser-induced population transfer by adiabatic passage techniques," Annu. Rev. Phys. Chem. **52**(1), 763–809 (2001).
[35]I. E. Gordon, L. S. Rothman, R. J. Hargreaves, R. Hashemi, E. V. Karlovets, F. M. Skinner, E. K. Conway, C. Hill, R. V. Kochanov, Y. Tan, P. Wcisło, A. A. Finenko, K. Nelson, P. F. Bernath, M. Birk, V. Boudon, A. Campargue, K. V. Chance, A. Coustenis, B. J. Drouin, J.-M. Flaud, R. R. Gamache, J. T. Hodges, D. Jacquemart, E. J. Mlawer, A. V. Nikitin, V. I. Perevalov, M. Rotger, J. Tennyson, G. C. Toon, H. Tran, V. G. Tyuterev, E. M. Adkins, A. Baker, A. Barbe, E. Canè, A. G. Császár, A. Dudaryonok, O. Egorov, A. J. Fleisher, H. Fleurbaey, A. Foltynowicz, T. Furtenbacher, J. J. Harrison, J.-M. Hartmann, V.-M. Horneman, X. Huang, T. Karman, J. Karns, S. Kassi, I. Kleiner, V. Kofman, F. KwabiaTchana, N. N. Lavrentieva, T. J. Lee, D. A. Long, A. A. Lukashevskaya, O. M. Lyulin, V. Yu. Makhnev, W. Matt, S. T. Massie, M. Melosso, S. N. Mikhailenko, D. Mondelain, H. S. P. Müller, O. V. Naumenko, A. Perrin, O. L. Polyansky, E. Raddaoui, P. L. Raston, Z. D. Reed, M. Rey, C. Richard, R. Tóbiás, I. Sadiek, D. W. Schwenke, E. Starikova, K. Sung, F. Tamassia, S. A. Tashkun, J. Vander Auwera, I. A. Vasilenko, A. A. Vigasin, G. L. Villanueva, B. Vispoel, G. Wagner, A. Yachmenev, and S. N. Yurchenko, "The HITRAN2020 molecular spectroscopic database," J. Quant. Spectrosc. Radiat. Transfer **277**, 107949 (2022).
[36]M. J. Weida and D. J. Nesbitt, "Collisional alignment of CO_2 rotational angular momentum states in a supersonic expansion," J. Chem. Phys. **100**(9), 6372–6385 (1994).
[37]J. P. C. Kroon, H. A. J. Senhorst, H. C. W. Beijerinck, B. J. Verhaar, and N. F. Verster, "Rabi oscillations in the optical pumping of a metastable neon beam with a cw dye laser," Phys. Rev. A **31**(6), 3724–3732 (1985).
[38]P. Atkins and J. De Paula, *Physical Chemistry*, 9th ed. (W. H. Freeman and Company, 2010).